Journal of Imaging Science and Technology® 55(2): 020504-1–020504-6, 2011.

Four Different Crystals Derived from a Novel Yellow Pyrazolyl Azo Pigment

Hiroki Shibata and Jin Mizuguchi▲
Department of Applied Physics, Yokohama National University, Yokohama 240-8501, Japan
E-mail: mizu-j@ynu.ac.jp

Abstract. *Four different crystals are presented in the present article that are derived from a novel yellow pyrazolyl azo pigment used for ink jet inks. This compound exhibits a good pigmentary performance in light and heat stability but rather poor in solvent fastness. X-ray structure analysis has been carried out in order to improve the present drawback from the structural point of view. The authors have unexpectedly isolated two kinds of five-coordinate bisazo Na complexes of the cis form (space group:* P-1*) as well as one Na-free monoazo compound (space group:* C2/c*). The formation of the Na complex is found to be caused by* $NaNO_2$ *used for the preparation of diazo components. Then, the authors tried to eliminate the sodium atom from the Na complex using hydrochloric acid in an attempt to develop a better pigment that assumes a trans configuration. The present Na-free compound in the trans form is found to crystallize in space group* P-1 *and is characterized by good solvent fastness in addition to the light and heat stability of the original title compound. © 2011 Society for Imaging Science and Technology.*
[DOI: 10.2352/J.ImagingSci.Technol.2011.55.2.020504]

INTRODUCTION

Azo pigments are widely used in imaging and printing industries because of their versatile colors, high tinctorial strength, as well as their low price.[1] Therefore, the azo compounds are by far the largest group of colorants with respect to number and production volume of currently marketed dyes and pigments. However, azo pigments are generally inferior in light, heat, and solvent fastness to phthalocyanines (blue), peryleneimides (vivid red via maroon to black), quinacridones (red and magenta), and pyrrolopyrroles (red), although considerable effort has been directed to improve these properties. On this account, azo pigments have commercial significance mainly for yellow. However, even today, there exist no high-performance yellow pigments that meet all pigmentary requirements, especially for ink jet inks.

Quite recently, some novel azo pigments have been reported by Nagata and Tateishi which include 2,6-bis { 5-amino-3-*tert*-butyl-4-[(3-methyl-1,2,4-thiadizol-5-yl) - diazeneyl]-1*H*-pyrazol-1-yl } - 1,3,5 - triazin - 4 (1*H*)-one[2] [B-PAT of the *cis* form: Figure 1(a)], whereas no description was made for its *trans* form [Fig. 1(b)]. In fact, B-PAT is found to exhibit a good pigmentary performance with respect to light and heat stability but rather poor solvent fastness. Then, an attempt was made in the present investigation to improve the above drawback from the standpoint of the crystal structure. In the process of growing single crystals from solution, we have unexpectedly isolated three kinds of single crystals: two bisazo and one monoazo compounds, indicating that the reaction product (assumed B-PAT) is not a pure material but a mixture of monoazo and bisazo compounds. To our even greater surprise, the bisazo compounds are found to include Na atoms and form five-coordinate Na complexes in a *cis* fashion [Na-containing B-PAT:[3,4] Figure 2(a)], whereas the monoazo compound is Na-free [M-PAT:[5] Fig. 2(b)]. Then, we wondered and asked ourselves where the Na atom comes from, how the Na atom is included in B-PAT, and why the Na complex crystallizes in a *cis* fashion that is less stable than the *trans* one. The formation of the Na complex is found to be caused by $NaNO_2$ used for the preparation of diazonium salts and the Na atom then bridges two monoazo moieties by force in a *cis* fashion. However, the integration of Na atoms derived from $NaNO_2$ in the azo moiety has never been reported in the long history of azo pigments.[1] At this moment, it struck us that we could prepare a structurally more stable *trans* form of B-PAT [Fig. 1(b)] by eliminating the Na atom from the Na complex, and this compound is expected to possess all desirable pigmentary characteristics. In fact, we could eliminate the Na atom using hydrochloric acid and isolate Na-free B-PAT in the *trans* form.[6] As expected, Na-free B-PAT in the *trans* form is found to possess high solvent fastness in addition to the light and heat stability of the original title compound.

The present article is a summary of the four different crystals derived from the assumed B-PAT [Fig. 1(a)] and describes how these compounds came to exist and how we arrived at the promising Na-free B-PAT of the *trans* form. The electronic structure will shortly be reported together with pigmentary characteristics.

EXPERIMENT

Preparation of B-PAT and Na-Free B-PAT of the trans Form

The assumed B-PAT [Fig. 1(a)] (i.e., the mixture of monoazo and bisazo compounds) was synthesized in accordance with a procedure described in the patent: [example 1 (0162)].[2] The diazonium salt was prepared by reaction of 5-amino-3-methyl-1,2,4-thiadiazole with $NaNO_2$. The salt was then coupled with 4,6-bis(5-amino-3-*tert*-butyl-1*H*-

---

▲IS&T Member.

Received Aug. 12, 2010; accepted for publication Nov. 29, 2010; published online Feb. 25, 2011.
1062-3701/2011/55(2)/020504/6/$20.00.

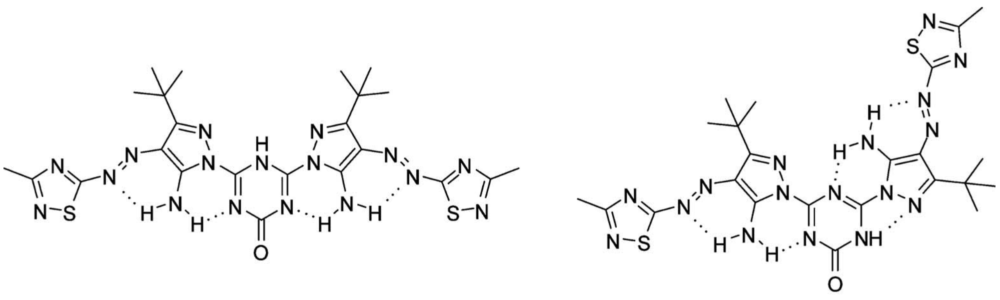
(a) (b)

Figure 1. Structure of B-PAT: (a) *cis* form {2,6-bis{5-amino-3-*tert*-butyl-4-[(3-methyl-1,2,4-thiadizol-5-yl) diazeneyl]-1*H*-pyrazol-1-yl}-1,3,5-triazin-4(1*H*)-one} and (b) *trans* form {4,6-bis{5-amino-3-*tert*-butyl-4-[(3-methyl-1,2,4-thiadizol-5-yl)diazeneyl]-1*H*-pyrazol-1-yl}-1,3,5-triazin-2(1*H*)-one}. Intramolecular hydrogen bonds are designated by dotted lines.

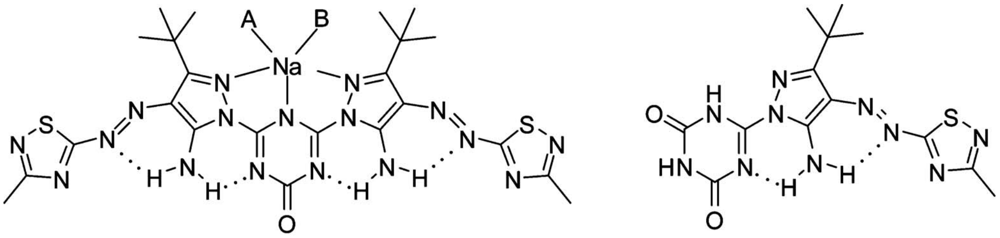
(a) (b)

Figure 2. Structure of the isolated monoazo and bisazo compounds: (a) Na-containing B-PATs of the *cis* form (B-PAT I with A=methanol and B=phenol: B-PAT II with A=water and B=NMP) and (b) Na-free M-PAT. Intramolecular hydrogen bonds are designated by dotted lines.

pyrazole-1-yl)-1,3,5-triazine-2-ol. The elementary analysis gave the result of C: 37.17%, H: 5.10%, N: 31.97%, S: 8.34%, and Na: 2.69%, whereas no analytical result was presented in the patent. The ratio of Na-containing B-PAT to Na-free M-PAT was about 4:1 according to the present analysis. On the other hand, Na-free B-PAT of the *trans* form was prepared by addition of HCl with 30 times molar equivalent to a B-PAT-saturated solution in *N*-methyl-2-pyrrolidone (NMP). The product was instantaneously precipitated upon dissolution of HCl, isolated by filtration, and washed with water. Elemental analysis gave the formula of $C_{23}H_{29}N_{17}OS_2 \cdot H_2O$ which is in good agreement with the theoretical value of B-PAT (M_w:$C_{23}H_{29}N_{17}OS_2=623.72$) being nonwater. In addition, mass spectrum gave the parent peak of 624 for B-PAT together with some small fractions.

Crystal Growth

Single crystals of Na-containing B-PAT I of the *cis* form were grown by recrystallization from a mixed solution of methanol and phenol (1:1 in molar ratio) prepared at 80°C. Needle shaped crystals were obtained in a closed system saturated with methanol vapor after standing for one week. Similarly, single crystals of Na-containing B-PAT II of the *cis* form and Na-free M-PAT were obtained from a solution in NMP prepared at 100°C. After standing for one week, single crystals were obtained in the form of needles for both Na-containing B-PAT II and M-PAT. On the other hand, the crystal growth of Na-free B-PAT of the *trans* form was extremely difficult. After many unsuccessful trials, needle-shaped single crystals could only be obtained from a chloroform solution.

Structure Analysis

All crystals appeared to include solvents except Na-free B-PAT in the *trans* form; reflection data were collected at −180°C (or at −120°C for Na-free B-PAT) on an R-AXIS RAPID-F diffractometer from Rigaku using Cu $K\alpha$ as the radiation source ($\lambda=1.5418$ Å). In all analyses, the structure was solved by direct methods (SIR2004[7]) and refinement was carried out by the full-matrix least-squares method, F^2 (SHELXL97[8]).

It was an extremely difficult task to solve the structure of Na-containing B-PATs of the *cis* form because we never thought at all of the inclusion of a Na atom in B-PAT [Fig. 1(a)] that derives from $NaNO_2$. In fact, no reports of the Na inclusion have been published in the long history of azo pigments.[1] At the beginning of the present analysis, we easily found major density peaks on Fourier maps which correspond to a bisazo structure of the *cis* structure. However, there remained a relatively strong density peak in the center of the molecule that has, however, an extremely small temperature factor. All our trials to assign the peak to oxygen, carbon, and nitrogen atoms were in vain. Finally, we were obliged to think of the existence of a monovalent or divalent metal such as Na or Mg in consideration of the small temperature factor which is typical of metals. The Na assignment was actually the clue to the successful determination of the structure.

Table I. Molecular orbital calculations for *cis* or *trans* B-PAT's and Na-containing *cis* B-PAT's.

	Heat of formation (kJ/mol)	Dipole moment (*D*)
cis B-PAT	1448.0	2.6
trans B-PAT	1422.5	2.3
Na-containing *cis* B-PAT I	926.1	12.9
Na-containing *cis* B-PAT II	770.0	16.0

Molecular Orbital Calculations

Semiempirical molecular orbital (MO) calculations were carried out on B-PATs and M-PAT using MOPAC2009.[9] Geometry was optimized with the AM1 Hamiltonian, and the spectroscopic calculations were made using ZINDO program integrated in the QUANTUM CACHE, Version 3.2 package.[10]

RESULTS AND DISCUSSION

MO Calculations

We discuss first the stability of the *cis* and *trans* forms of B-PAT, together with that of Na-containing B-PAT. This serves as the basis for discussions of the crystal structure described below.

Table I lists the results of the MO calculations, showing the heat of formation and the dipole moment for *cis* B-PAT [Fig. 1(a)], *trans* B-PAT [Fig. 1(b)], Na-containing *cis* B-PAT I (with A = methanol and B = phenol in Fig. 2), and B-PAT II (with A = water and B = NMP). Obviously, the heat of formation of the *trans* form (1422.5 kJ/mol) is lower than that of the *cis* form (1448.0 kJ/mol) by about 25.5 kJ/mol, indicating that the *trans* form is more stable than the *cis* one. However, the situation drastically reverses when the Na atom is integrated into *cis* B-PAT: 926.1 and 770.0 kJ/mol for Na-containing *cis* B-PATs I and II, respectively. This explains why the Na-containing B-PAT of the *cis* form exists in reality as the most stable structure.

Crystal Structure

Table II details the crystallographic parameters for Na-containing B-PAT I of the *cis* form (with A = methanol and B = phenol in Fig. 2), B-PAT II of the *cis* form (with A = water and B = NMP), Na-free B-PAT of the *trans* form, and Na-free M-PAT. Among these, only Na-free B-PAT contains no solvents, while the rest are solvated crystals. M-PAT is characterized by a space group of $C2/c$, while the others possess P-1. The inclusion of the Na atom comes as a great surprise. The formation of Na complexes is found to be caused by $NaNO_2$ used for the preparation of diazo components, and the Na atom bridges two monoazo moieties in a *cis* fashion, as described below.

MOLECULAR CONFORMATION AND ARRANGEMENT

Na-Containing B-PAT I of the cis Form

Figure 3 shows the *ORTEP* plot of Na-containing B-PAT I of the *cis* form which includes three full phenol molecules and two half molecules in the asymmetric unit. Four of these are hydrogen-bonded to the N atom of the 1,2,4-thiadiazol ring through OH···N hydrogen bonds, while the fifth phenol molecule remains free. It is remarkable to note that the central Na atom bridges two monoazo moieties in a *cis* fashion

Table II. Crystallographic parameters for four different crystals derived from the assumed B-PAT.

	Na-containing B-PAT I of the *cis* form[a]	Na-containing B-PAT II of the *cis* form[b]	Na-free B-PAT of the *trans* form[c]	Na-free M-PAT[d]
Molecular formula	$C_{30}H_{38}N_{17}O_3S_2Na\cdot 4(C_6H_6O)$	$C_{28}H_{39}N_{18}O_3S_2Na\cdot C_5H_9NO$	$C_{23}H_{29}N_{17}OS_2$	$C_{13}H_{16}N_{10}O_2S\cdot C_5H_9NO\cdot H_2O$
Molecular weight	1148.3	861.98	623.72	493.54
Crystal system	Triclinic	Triclinic	Triclinic	Monoclinic
Space group	P-1	P-1	P-1	$C2/c$
Z	2	2	2	8
a (Å)	8.389,64(15)	12.110,0(8)	6.756,1(12)	27.828,3(5)
b (Å)	18.878,0(3)	13.778,1(9)	14.054(2)	7.026,90(10)
c (Å)	20.406,0(4)	14.669,5(9)	16.203(3)	26.441,7(4)
α (deg)	114.103,0(7)	63.125(3)	83.924(6)	···
β (deg)	96.580,0(8)	89.298(3)	83.276(7)	91.343,0(7)
γ (deg)	95.650,0(8)	73.534(3)	79.140(7)	···
V (Å^3)	2,892.83(9)	2,074.4(2)	1,495.0(4)	4,582.69(13)
D_x (g/cm^3)	1.318	1.38	1.385	1.431
R_1	0.0726	0.1478	0.1373	0.049,3

[a] Reference 3.

[b] Reference 4.

[c] Reference 6.

[d] Reference 5.

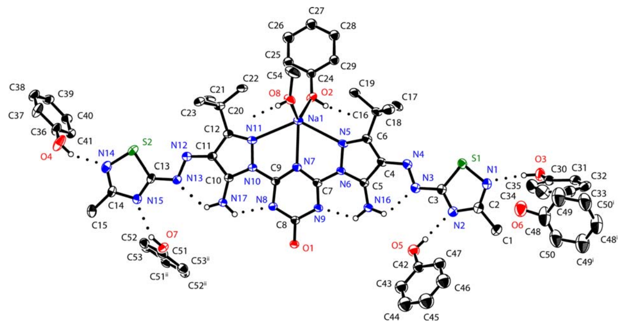

Figure 3. ORTEP plot for Na-containing B-PAT I of the *cis* form. Intermolecular and intramolecular hydrogen bonds are designated by dotted lines.

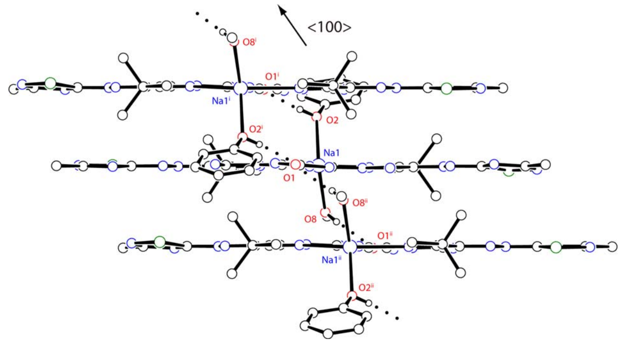

Figure 4. Hydrogen-bond network of Na-containing B-PAT I of the *cis* form along the stacking *a* axis. Symmetry codes: (i) $(-x,-y,-z)$ and (ii) $(-1-x,-y,-z)$. Intermolecular hydrogen bonds are designated by dotted lines.

to make the molecule entirely flat (mean deviation from the least-squares plane with a methyl group from the *tert*-butyl substituent on the pyrazol ring above and below that plane: 0.0524 Å). Additionally, the four intramolecular NH···N hydrogen bonds also contribute to the planarity of the system. The occurrence of the *cis* form is quite unusual because the *trans* form of the Na-free structure as formed by free rotation around C7-N6 or C9-N10 is more stable according to the MO calculations (Table I). Nevertheless, the Na coordination serves as the driving force to form the *cis* structure, as suggested by the MO calculations. The Na^+ cation is bound to three N atoms (N5, N7, and N11) of the triazine ligand, two from each pyrazole ring and one from the central deprotonated triazine ring system. Furthermore, the O atoms of phenol and methanol molecules are also coordinated to the Na atom, generating a five-coordinate Na-bisazo complex. The integration of the Na atom is due largely to the favorable distance of the Na position from N5, N7, and N11: $\mathrm{Na1-N5}=2.644(3)$, $\mathrm{Na1-N7}=2.420(3)$, and $\mathrm{Na1-N11}=2.642(3)$ Å. The distances of Na1–N5 and Na1–N11 are nearly equal, reflecting that the angles of N5/Na1/N7 and N7/Na1/N11 are 65.04(8)° and 65.51(8)°, respectively. The present Na-N distance of about 2.42–2.64 Å is slightly longer than the value of 2.4381(9) Å reported in a Fe complex of the bisazo compound, where the molecule forms a centrosymmetric dimer with two octahedral Fe^{III} units linked by two bridging five-coordinate Na^{I} cations.[11]

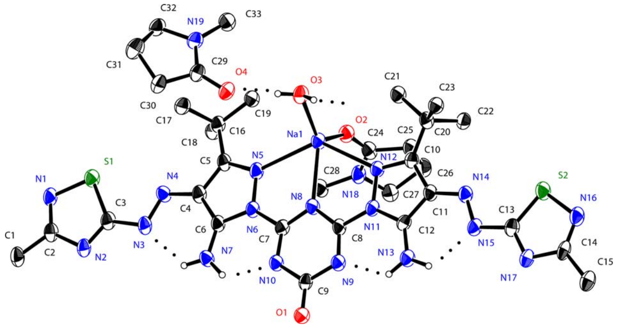

Figure 5. ORTEP plot for Na-containing B-PAT II of the *cis* form. Intermolecular and intramolecular hydrogen bonds are designated by dotted lines.

Figure 4 illustrates the molecular stack of Na-containing B-PAT I of the *cis* form along the *a* axis. The methanol and phenol ligands to the Na atom are positioned above and below the bisazo skeleton. The polar bisazo molecules are arranged alternately in such a way as to effectively cancel their dipole moments to lower the lattice energy. In addition, two stacked columns are formed that are composed of the central Na(I) atom sandwiched by alternating two kinds of intermolecular hydrogen bonds: O (carbonyl oxygen:O1^{ii})···O-H (methanol: O8)/Na1/O-H (phenol:O2)···O (carbonyl oxygen: O1^{i}) [symmetry codes: (i) $(-x,-y,-z)$ and (ii) $(-1-x,-y,-z)$]. This forms two one-dimensional polymer chains per molecule and assures a high thermal stability of the compound.

Na-Containing B-PAT II of the cis Form

Figure 5 shows the ORTEP plot of Na-containing B-PAT II of the *cis* form with one solvated NMP. The geometry of the present five-coordinate Na complex is quite similar to Na-containing B-PAT I except the ligands arising from the solvent (i.e., coordinating solvents). The Na^+ cation is bound to three N atoms (N5, N8, and N12) of the triazine ligand, two from each pyrazole ring and one from the central deprotonated triazine ring system. O2 from NMP and O3 from (water) complete the five-coordinate NaN_3O_2 coordination environment. In addition, O4 of solvated NMP is hydrogen bonded to the H atom of the water molecule. The water present is presumably derived from moisture in air or traces of water included in NMP.

Figure 6 illustrates the side view of the complex conformation, showing the arrangement of NMPs and water with respect to the triazinide plane. In addition, O4 is hydrogen bonded to H13A^{i} and H13B^{i} of the amino group of the neighboring molecule through two intermolecular hydrogen bonds: O4···H13A-N13 and O4···H13B-N13 bonds. [symmetry code: (i) $(1-x,2-y,1-z)$]. This bridges two Na complexes to form a dimer, as shown in Figure 7, together with two additional intermolecular O···HO hydrogen bonds between the carbonyl O atom of the triazine ring of one molecule and the H atom of the water molecule of the neighboring one. These dimers are stacked along ⟨100⟩.

Na-Free B-PAT of the trans Form

Figure 8 shows the ORTEP plot of Na-free B-PAT of the

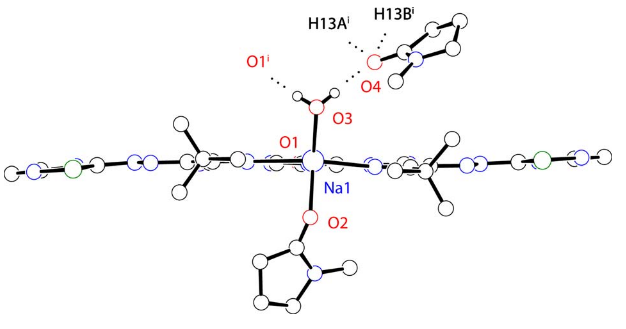

Figure 6. Side view of Na-containing B-PAT II of the *cis* form. Symmetry code: (i) $(1-x, 2-y, 1-z)$. Intermolecular hydrogen bonds are designated by dotted lines.

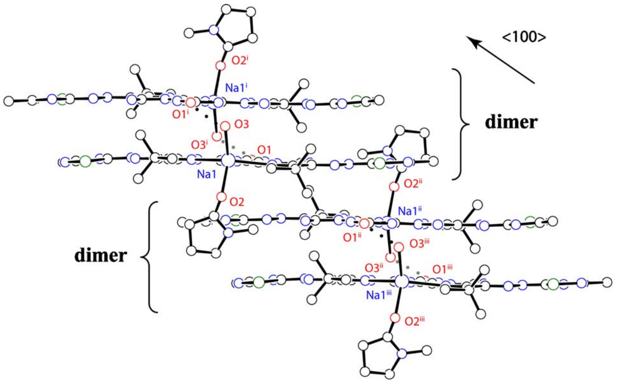

Figure 7. Dimers of Na-containing B-PAT II of the *cis* form along the stacking *a* axis. Symmetry codes: (i) $(1-x, 2-y, 1-z)$, (ii) $(-x, 2-y, 1-z)$, and (iii) $(-1+x, y, z)$. Intermolecular hydrogen bonds are designated by dotted lines.

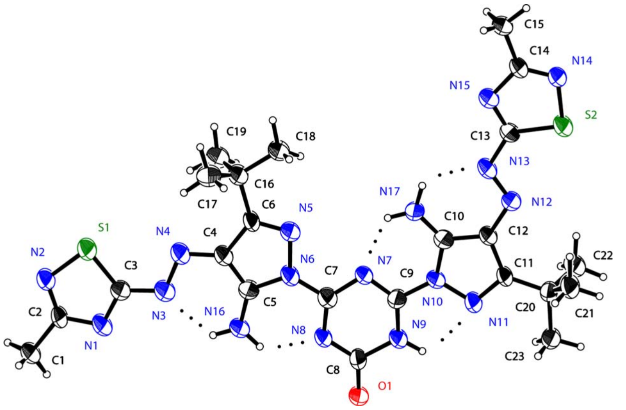

Figure 8. ORTEP plot for Na-free B-PAT of the *trans* form. Intramolecular hydrogen bonds are designated by dotted lines.

trans form. There are five NH···N intramolecular hydrogen bonds formed between the NH of the amino group of the pyrazol ring and the N atom of the azo bond: N16-H16M···N3, N16-H16N···N8, N17-H17M···N13, N17-H17N···N7, and N9-H9···N11. The five intramolecular NH···N hydrogen bonds contribute to the planarity of the system.

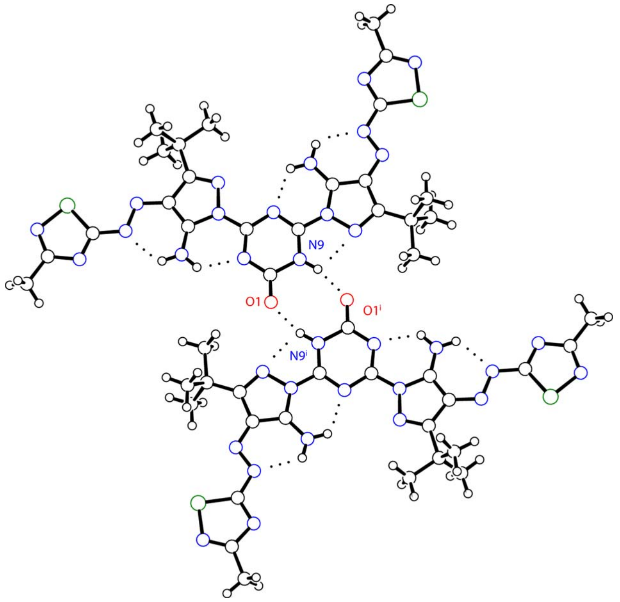

Figure 9. Hydrogen-bonded dimers of Na-free B-PATs of the *trans* form. Symmetry code: (i) $(1-x, 2-y, 1-z)$. Intermolecular and intramolecular hydrogen bonds are designated by dotted lines.

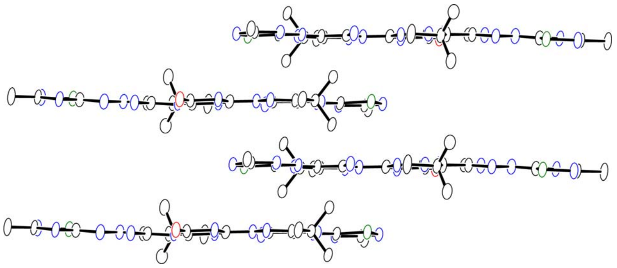

Figure 10. Molecular stack of Na-free B-PATs of the *trans* form.

Figure 9 illustrates the in-plane dimer structure formed by two NH···O intermolecular hydrogen bonds: O1···H9^{i}-N9^{i} and N9-H9···O1^{i} bonds [symmetry code: (i) $(1-x, 2-y, 1-z)$]. The formation of dimers doubles the molecular unit to significantly stabilize the solid state. The present dimer is formed without any intermediator such as solvents, whereas that of Na-containing B-PAT II of the *cis* form is formed between two stacked molecules through coordinating solvents (Fig. 7). The molecules are stacked with a small overlap at one corner of the molecule, as shown in Figure 10. The present Na-free B-PAT of the *trans* form is found to be quite resistant to light, heat, and solvent, as will shortly be reported elsewhere.

Na-Free M-PAT

Figure 11 shows the ORTEP plot of Na-free M-PAT. The formation of three intramolecular hydrogen bonds—N2-H2···N5, N10-H10M···N7, and N10-H10N···N3—stabilizes a planar conformation of the molecule. The water molecule is hydrogen bonded to the O3A atom of the NMP molecule. In turn, the O4 atom is hydrogen bonded to the H10M-N10 amino group of the monoazo skeleton. In addition, the O4-H4B group is weakly hydrogen-bonded to both N7 and N8. At both ends of the long molecular axis of the main molecule, the molecules are

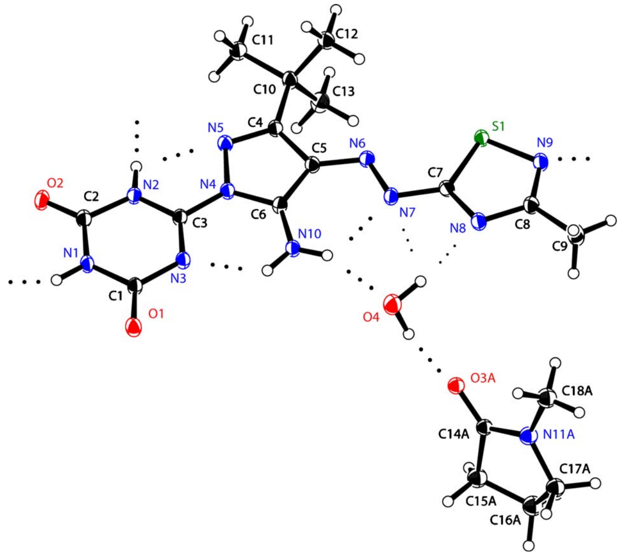

Figure 11. ORTEP plot for Na-free M-PAT. Intermolecular and intramolecular hydrogen bonds are designated by dotted lines.

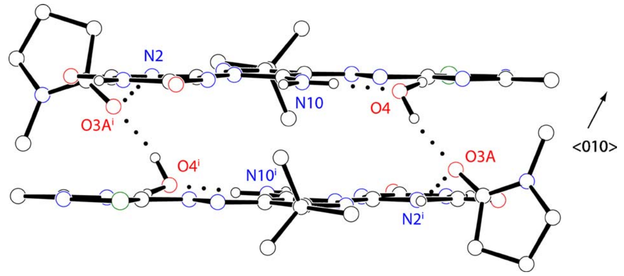

Figure 12. Dimer of Na-free M-PATs. Symmetry code: (i) $(1/2-x, 1/2-y, 1-z)$. Intermolecular hydrogen bonds are designated by dotted lines.

arranged in a head-to-tail fashion on the molecular planewith intermolecular N1-H1···N9 hydrogen bonds. These form a one-dimensional polymer chain on the molecular plane along the long molecular axis: $\langle 110\rangle$ or $\langle 1\bar{1}0\rangle$ direction.

As shown in Figure 12, the monoazo molecules are alternately stacked along the $\langle 010\rangle$ direction in such a way to cancel their dipole moments so as to electrostatically stabilize themselves in the crystal. Each alternating pair is linked through a set of three-consecutive intermolecular hydrogen bonds. On one side of the molecule: N2-H2 (triazine ring)···O3A^i (NMP), O3A^i (NMP)···H4A^i-O4^i (water), and O4^i (water)···H10M^i-N10^i (amino group) [symmetry code: (i) $(1/2-x, 1/2-y, 1-z)$]. An equivalent set of H-bonding interactions is found at the opposite sides of the molecules.

CONCLUSIONS

Structure analysis has been carried out on four different crystals derived from the title compound. The conclusions can be summarized as follows.

1. The previously reported B-PAT is found to be a mixture of monoazo and bisazo compounds.
2. Two kinds of Na-containing B-PAT of the *cis* form and Na-free M-PAT were isolated as single crystals. $NaNO_2$ used for the preparation of diazonium components is responsible for the Na-complex formation.
3. Na-containing B-PAT is a five-coordinate Na complex of the *cis* form. The central Na atom bridges two monoazo moieties together to give a *cis* arrangement. Elimination of the Na atom yields a Na-free B-PAT of the *trans* form.
4. Na-containing or Na-free B-PATs as well as Na-free M-PAT are characterized by the formation of NH···N intramolecular hydrogen bonds which make the molecule entirely flat. Na-containing B-PAT I forms two one-dimensional polymer chains per molecule along the stacking axis, whereas Na-containing B-PAT IIs are dimerized through solvent ligands along the stacking axis as well. On the other hand, two Na-free B-PATs of the *trans* arrangement form an in-plane dimer through two NH···O intermolecular hydrogen bonds. Na-free M-PAT is characterized by the formation of one dimensional polymer due to NH···N intermolecular hydrogen bonds arranged in a “head-to-tail” fashion.
5. Na-free B-PAT is found to exhibit good solvent fastness in addition to the light and heat stability of the original title compound. Details on this subject as well as the electronic structure will shortly be reported elsewhere.

REFERENCES

[1] M. Herbst and K. Hunger, *Industrial Organic Pigments*, 3rd ed. (VCH, Weinheim, 2004).

[2] Y. Nagata and K. Tateishi, Preparation of azo pigments, Japan Patent 2009-73978 (2009).

[3] H. Shibata and J. Mizuguchi, “(2,6-bis{5-amino-3-*tert*-butyl-4-[(3-methyl-1,2,4-thiadiazol-5-yl)diazenyl]-1*H*-pyrazol-1-yl}-4-oxo-1,4-dihydro-1,3,5-triazin-1-ido) methanol(phenol)sodium phenol tetrasolvate”, Acta Crystallogr., Sect. E: Struct. Rep. Online **66**, m463–m464 (2010).

[4] H. Shibata and J. Mizuguchi, “(2,6-bis{5-amino-3-*tert*-butyl-4-[(3-methyl - 1, 2, 4 - thiadiazol-5-yl) diazenyl] -1*H*-pyrazol-1-yl} -4-oxo-1,4-dihydro-1, 3, 5 -triazin -1- ido) *N*-methyl-2-pyrrolidone (water) sodium *N*-methyl-2-pyrrolidone”, X-ray Structure Analysis Online **26**, 63–64 (2010).

[5] H. Shibata and J. Mizuguchi, “6-{5-amino-3-*tert*-butyl-4-[(*E*)-(3-methyl-1,2,4-thiadiazol-5-yl) diazenyl] -1*H*-pyrazol-1-yl} -1,3,5-triazine-2,4-(1*H*,3*H*)-dione-1-methylpyrrolidin-2-one-water”, Acta Crystallogr., Sect. E: Struct. Rep. Online **66**, o944–o945 (2010).

[6] H. Shibata and J. Mizuguchi, “Crystal structure of 4,6-bis{5-amino-3-*tert*-butyl-4-[(3-methyl-1,2,4-thiazol-5-yl)diazenyl] -1*H*-pyrazol-1-yl}-1,3,5-triazin-2(1*H*)-one of the *trans* form”, X-ray Structure Analysis Online **26**, 67–68 (2010).

[7] M. C. Burla, “SIR2004: An improved tool for crystal structure determination and refinement”, J. Appl. Crystallogr. **38**, 381–388 (2005).

[8] G. M. Sheldrick, “A short history of SHELX”, Acta Crystallogr., Sect. A: Found. Crystallogr. **64**, 112–122 (2008).

[9] J. J. P. Stewart, MOPAC2009 (Stewart Computational Chemistry, Colorado Springs, CO, 2008).

[10] QUANTUM CACHE, Version 3.2 (Fujitsu, Ltd., Kanagawa, Japan, 1999).

[11] Y. Sato, U. Kazuya, and J. Mizuguchi, “Diacetonitriletetrakis {μ_2 -3-anilinocarbonyl-1- [(5-chloro-2-oxidophenyl) diazenyl] -2-naphtholato } tetraaquadiiron (III) disodium (I) dehydrate”, Acta Crystallogr., Sect. E: Struct. Rep. Online **64**, m240–m241 (2008).